Available online at www.sciencedirect.com
SCIENCE DIRECT®
PERGAMON
International Journal of Heat and Mass Transfer 46 (2003) 2957–2965
International Journal of HEAT and MASS TRANSFER
www.elsevier.com/locate/ijhmt

# Experimental study of unsteady convective boiling in heated minichannels

D. Brutin *, F. Topin, L. Tadrist

*Laboratoire IUSTI, UMR 6595 CNRS/Université de Provence, Ecole Polytechnique Universitaire de Marseille, Technopôle de Château-Gombert-5, rue Enrico Fermi, 13453 Marseille, France*

Received 3 April 2002; received in revised form 24 January 2003

**Abstract**

Convective boiling in narrow channels may under specific conditions display an unsteady behavior. An experimental set-up has been elaborated to investigate heat and mass transfer and to analyze two-phase flow instabilities in rectangular microchannels with a hydraulic diameter of 889 μm. Depending on the operating conditions two types of behavior are observed: a steady state characterized by pressure drop fluctuations with low amplitudes (from 0.5 to 5 kPa/m) and no characteristic frequency; a non-stationary state of two-phase flow. The pressure signals exhibit fluctuations with high amplitudes (from 20 to 100 kPa/m) and frequencies ranging from 3.6 to 6.6 Hz. Steady and unsteady thermo-hydraulic behaviors depending on the two control parameters (heat flux and mass velocity) are analyzed and given in this paper.


*Keywords:* Convective boiling; Minichannels; Instabilities

## 1. Introduction

Microsystems have been widely explored and developed in the past ten years due to their low cost and high potential applications in many fields such as space, communication, biology and industry [1]. Industrial manufacturing conceives such complex devices which use or transport fluids. The understanding of flow behavior on a microscale, down to a few micrometers, has not followed the fast development of such microsystems. On such small scales, phenomena such as interfacial ones which are often negligible in classical flows become dominant. Although, when a phase change occurs, problems related to the starting scale of bubbles arise due to the submillimetric dimensions of such a system's channels. So, the heat and mass transfer studies are being widely developed to allow industrial application development.

Numerous studies have been carried out on boiling since the sixties; some have focussed on instabilities in two-phase systems which can lead to flow excursions or flow oscillations [2–5]. These unsteady behaviors can induce a boiling crisis (dryout, burnout…) and cause mechanical damage. In microchannels in which the hydraulic diameter is below the capillary length, surface tension effects are not negligible unlike classical channels. The two-phase flow dynamic is modified by the liquid–vapor velocity slip, for example, which is directly related to the surface tension. Also, the temperature and velocity gradients near the channel walls are much more significant due to the microchannel dimensions; this implies that the boiling phenomena must differ from those in a channel of large dimensions, where the wall proximity will not affect the bubble growth and evolution. Recent developments in microsystems such as micro-heat exchangers, microfluidics have opened up a new field of research both in monophasic studies (flow pattern, friction factor…) and in biphasic studies

* Corresponding author. Tel.: +33-4-91-10-68-68; fax: +33-4-91-10-69-69.
*E-mail address:* david.brutin@polytech.univ-mrs.fr (D. Brutin).

0017-9310/03/$ - see front matter 
doi:10.1016/S0017-9310(03)00093-0

**Nomenclature**

| | |
|---|---|
| $A$ | cross section ($m^2$) |
| $Bo$ | Bond number |
| $d$ | distance (m) |
| $D_H$ | hydraulic diameter (m) |
| $e$ | thickness (m) |
| $F$ | oscillation frequency (Hz) |
| $l$ | width (m) |
| $L$ | length (m) |
| $L_V$ | heat of vaporization ($J\,kg^{-1}$) |
| $P$ | pressure (Pa) |
| $P_W$ | power (W) |
| $Q_W$ | heat flux ($W\,m^{-2}$) |
| $Q_M$ | mass velocity ($kg\,m^{-2}\,s^{-1}$) |
| $Re$ | Reynolds number |
| $T$ | temperature (°C) |
| $U$ | fluid velocity ($m\,s^{-1}$) |

*Greek symbols*

| | |
|---|---|
| $\chi$ | quality |
| $\delta$ | fluctuating component |
| $\Delta$ | difference |
| $\mu$ | dynamic viscosity (Pa s) |
| $\varrho$ | density ($kg\,m^{-3}$) |
| $\sigma$ | surface tension ($N\,m^{-1}$) |
| $\tau$ | transit time (s) |

*Subscripts and superscripts*

| | |
|---|---|
| Atm | atmospheric |
| B | biphasic |
| In | inlet |
| L | liquid |
| Out | outlet |
| Sat | saturation |
| V | vapor |
| W | wall |

(two-phase flow behavior, heat-exchange coefficient, boiling stability...). Concerning convective boiling in narrow channels, few papers deal with instabilities because this field is also under investigation [6,7]. Many types of instabilities can develop in flow boiling: flow excursion (or Ledinegg instability) is the most common one explained by a criterion [8]. A boiling crisis is also a static instability characterized by a wall temperature excursion and so by an ineffective removal of heat from the heated surface. Fundamental relaxation instability such as bumping, geysering or chugging is another static instability which can be described as a periodic process of super-heat and violent evaporation with possible expulsion and refilling. Dynamic instabilities such as acoustic wave, density wave or thermal oscillations can also occur and are characterized by other typical frequencies, amplitudes and physical mechanisms [9].

A state of art analysis on convective boiling in channels shows some interesting studies which have reported unsteady flow boiling [10–12]. Usually, the duct diameters investigated are of only a few millimeters, but some authors work with narrow channels such as Kew and Cornwell [13]. They highlighted an appearance threshold of the instability phenomena when the starting diameter of the bubble approaches the hydraulic diameter of the channel. In 1996, they proposed a model of pressure fluctuation within cylindrical channels, based on the displacement of a liquid slug surrounded by expanding vapor [14]. In 1998, Aligoodarz et al. [15] observed temperature fluctuations of the same order as the average overheating of the wall in channels of various sizes. Kennedy et al. [6] investigated boiling in tubes of an internal diameter down to 1.17 mm. They studied the onset of nucleate boiling (ONB) and onset of flow instability (OFI) in uniformly heated tubes cooled by subcooled water. They based the ONB and OFI determination on the pressure drop versus mass flow rate curves obtained for each fixed heat flux. They deduced that the experimental heat flux at the OFI is function of 90% of heat flux for bulk saturation and follows a linear evolution. A relationship between these two parameters seems, thereby, to exist but the choice of 90% by the authors is unclear. Peng and Wang [16] conducted single-phase and flow boiling experiments of some fluids and mixtures in rectangular microchannels of hydraulic diameter from 343 to 133 μm and triangular microchannels ranging from 600 to 200 μm. Unusual phase-change transport phenomena were observed by the authors; they try to explain such behavior through two new concepts of "evaporating space" and fictitious boiling". They deduced from their experiments that "nucleate boiling in microchannels having dimensions from several hundred to less than one micrometer is almost impossible". Jiang et al. [17] devised a transparent microchannel heat sink system to visualize the flow pattern and take temperature measurements during flow boiling. For the low power supplied to the fluid flow, they observed that local nucleation was possible but difficult to generate even for 40 μm hydraulic diameter channels. For intermediate power slugs flow develop and for high power supplied a steady annular flow mode was noticed. Chang and Yao [18] investigated pool boiling in vertical annuli from 2.58 mm down to 320 μm gap sizes and identified three boiling regimes

through flow pattern visualization correlated to the Bond number ($Bo$): isolated deformed bubble regime for $Bo < 1$ and low heat flux; coalesced deformed bubble regime also for $Bo < 1$ and high heat flux; and nucleation under slightly deformed bubbles when $Bo > 1$ and for high heat flux. In 1994, Wambsganss et al. [19] related flow pattern transitions to an RMS channel pressure drop and evidenced an increase in the RMS pressure drop in the plug-bubble flow regime followed by a further sharp increase when the slug flow regime occurs and then an RMS pressure drop decrease when the annular flow appears. Also, they related these RMS pressure variations to the flow visualization. During the bubble flow regime, as the mass quality, and consequently the RMS pressure drop, increases, the bubble size decreases. When the channel is full of bubbles they collapse, resulting in a slug flow pattern.

So, the next step is to have a better understanding of boiling in confined spaces; so to reduce the observation scale to only one microchannel. Globally, through the literature, it appears in microtubes non-intrusive measurements are hardly realizable whereas with a rectangular or even triangular cross section, it is possible to take measurement on one side and on the other either to have the heating surface or a visualization face. The fluid commonly used is water for its advantages of price and null toxicity. Some authors use R-113 for its low boiling temperature and so the low power supplied for boiling. The geometry commonly used is the rectangular one usually easy to instrument in pressure and temperature measurements. On such small scales (below 1 mm) it becomes difficult to take measurements without disturbing heat and mass transfers. The knowledge on microheat and mass transfer is embryonic and must be investigated through single and two-phase flow experiments to compare to macroscale laws currently used to predict either pressure drop, heat flux at OFI, heat exchange coefficient...

The aim of this paper is to analyze the two-phase flow behavior and the heat and mass transfer when steady and unsteady regimes occur in channels with a hydraulic diameter less than 1 mm. The objective is to acquire a better knowledge of elementary phenomena which control the heat and mass transfers during phase change on such small scale. First, the experimental set-up and the procedure will be described. Then, the different boiling states observed and their behavior will be presented through pressure, temperature and high speed video camera analysis.

## 2. Experimental set-up

The physical model is a rectangular microchannel heated at the rear face, through which an upward fluid passes. The heated liquid is $n$-pentane for which the physical properties are given in Table 1. The saturation temperature at atmospheric pressure, heat of vaporization and specific heat are quite small to allow boiling with low-power and low-temperature devices.

Table 1
$n$-Pentane liquid and vapor properties

| Conditions | | Value | Unit |
|---|---|---|---|
| 25 °C | $\sigma$ | $13.12 \times 10^{-3}$ | $N\,m^{-1}$ |
| 25 °C | $\mu_L$ | $2.23 \times 10^{-4}$ | $Pa\,s$ |
| | $\varrho_L$ | 621 | $kg\,m^{-3}$ |
| | $Cp_L$ | 2142 | $J\,kg^{-1}\,K^{-1}$ |
| 36 °C | $\varrho_V$ | 2.57 | $kg\,m^{-3}$ |
| | $\mu_V$ | $6.78 \times 10^{-6}$ | $Pa\,s$ |
| | $Cp_V$ | 1717 | $J\,kg^{-1}\,K^{-1}$ |
| 1010 hPa | $T_{Sat}$ | 36 | °C |
| 36 °C | $L_V$ | 382,450 | $J\,kg^{-1}$ |

### 2.1. Description

The experimental device (Fig. 1) is composed of four main parts: the channel, the condensation system, the injection device and the video acquisition device. We create a fluid flow using a peristaltic pump coupled with a buffer tank completely filled with liquid to reduce the mass flow rate fluctuations. The channel is heated using an electrical resistor connected to an electrical heater. The voltage and intensity supplied are controlled to calculate the heating power supplied to the channel. Experiments in single-phase flow allow by an energy balance to evidence heat losses under 5%. This setup allows us to control the fluid flow (mass flow rate) and the heating parameters (inlet temperature, heat power supplied). The test cells are rectangular channels with dimensions $(e, l, L)$ of $0.5 \times 4 \times 50$ and $0.5 \times 4 \times 200$ mm$^3$.

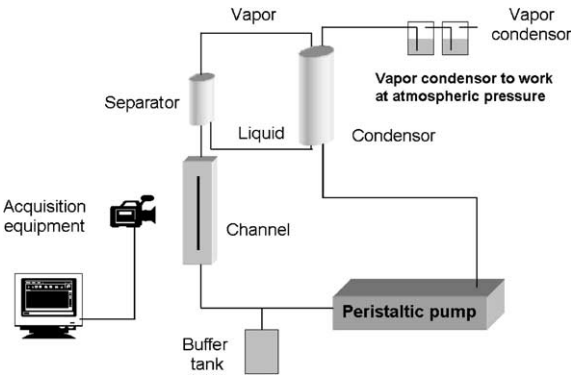


Fig. 1. Experimental set-up composed of the minichannel, the condensation devices, the injection devices and the acquisition system.

The channels are hollowed out of aluminum rods covered with *polycarbonate*® plates. An electrical resistance heater ensures heating of the channel's rear face while the transparent front face, which allows the observation of the flow patterns, is fixed with a thin calibrated adhesive tape. The fluid is introduced at the bottom of the channel at a constant flow rate using the peristaltic pump. Channels of different sizes are designed in order to highlight the influence of the channel's dimension on flow pattern and the thermo-hydraulic characteristics (the instability's appearance conditions, frequency...). Two versions of the $0.5 \times 4 \times 200$ mm$^3$ channel are made: the first channel is only equipped at the entrance and the exit with pressure and temperature tapping holes and its transparent front face is totally available for visualization whereas, the second channel is equipped like the first one plus through the transparent front face with pressure and temperature tapping holes to obtain the local thermo-hydraulic fluid state. The error margin after measurement of the channel geometry indicates a discrepancy of 0.84% in the hydraulic diameter and 0.5% in the channel length.

### 2.2. Temperature and pressure instrumentation

We use Sensym® SCX05DN pressure sensors of sensitivity: 0.57 Pa/μV. The pressure transducers are calibrated up to 50 kPa. The accuracy due to the electrical set-up is of 40 μV so the accuracy of the pressure signal is about 20 Pa. Temperature measurements are taken with K-type thermocouples with a diameter of 0.5 mm. The accuracy of the temperature measurements is 1 K. The data acquisition device is a National Instrument® PCI 6033E. Pressure and temperature measurements are placed at several locations along the main flow axis through the front face (Fig. 2). All measured data (temperature, pressure, flow rate) are simultaneously acquired. The acquisition frequency depends on the fluid state: for a steady state, the acquisition is at 20 Hz and for an unsteady one at 200 Hz.

### 2.3. Experimental procedure

The fluid inside the loop is heated to obtain boiling nucleation for a few minutes to eliminate the non-condensable gas by an opening in the loop. The fluid is then returned to standard conditions and the experiments are carried out using an established procedure. For a fixed mass flow rate and heat flux, temperature and pressure measurements are taken permanently at different scanning frequencies according to the observed phenomena dynamics. The heating power is stepped up; then the new state is investigated. This procedure is repeated until the maximum temperature technically acceptable for the microchannel is reached. This procedure is reproduced for each mass flow rate studied.

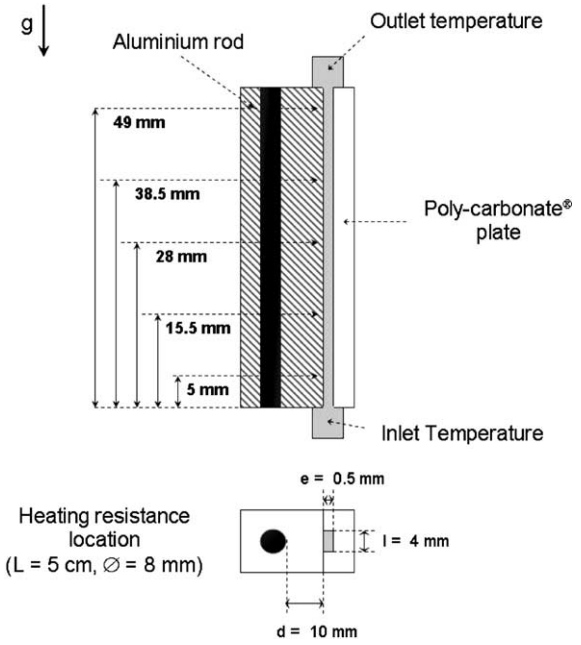


Fig. 2. Example of thermocouple location in a $0.5 \times 4 \times 50$ mm$^3$ heated minichannel.

All acquired data are post-processed. After identification of the stationary range of each point (mass flow rate, heat flux) the time averages of temperature and pressure are computed. The vapor quality and the pressure drop are deduced (Eq. (1)). The dynamics of the parameters are then analyzed (temperature and pressure). For each experimental condition, the frequency and amplitude fluctuations are computed.

$$\chi_V = \frac{1}{L_V}\left(\frac{4Q_W L}{\mu Re_L} - Cp_L(T_{Sat} - T_{In})\right) \quad (1)$$

## 3. Results

### 3.1. Fluid behavior description

Several thermo-hydraulic states are observed according to the operating conditions (mass flow rate, heat flux) independently of their variation mode. Thus, for a given mass flow rate for example 240 kg m$^{-2}$ s$^{-1}$ [$(e, l, L) = 0.5 \times 4 \times 50$ mm$^3$], according to the heat flux we observe the following: at a moderate heat flux (under $20 \times 10^4$ W m$^{-2}$), two steady zones coexist in the channel. At the bottom of the test cell, the fluid is liquid. Upstream, bubbles whose number and size vary with the operating conditions are observed (bubbly flow). Under these conditions, the temperature and the pressure remain steady and equal to their values of saturation at

the exit of the channel. Above a critical value of the heat flux ($38 \times 10^4$ W m$^{-2}$), an oscillatory regime appears. A fluctuation of the two-phase flow can be clearly observed in the channel. The phenomenon induces inlet and outlet fluctuations in pressures with given frequencies. Beyond a second critical heat flux ($50 \times 10^4$ W m$^{-2}$), this phenomenon disappears and a steady mode (film boiling) is observed again; a small fluid area at the bottom of the test cell is surmounted by a two-phase flow with a high vapor fraction. For data taken during an oscillatory mode, a spectral analysis of pressure signals is made in order to characterize the channel pressure losses. For some operating conditions, harmonics of second and higher order are observed. This typical behavior will be described in a further section.

### 3.2. Stability criteria

There is no theoretical criterion to distinguish steady and unsteady boiling. Experiments carried out show up these two behaviors through pressure analysis and visualization. A criterion is fixed, based on our observation. The steady state is defined by a low fluctuation amplitude <1 kPa and no characteristic oscillation frequency identified by spectrum analysis (the ratio of the peak amplitude divided by noise amplitude below 20). The unsteady state is defined by a high fluctuation amplitude >1 kPa and a characteristic oscillation frequency of a ratio higher than 20 (peak amplitude below noise amplitude).

### 3.3. Stability diagram

On the stability diagram (Fig. 3), the unsteady operating points characterized by the two parameters heat flux and mass flow rate are reported. The uncertainty in the heat flux mainly due to the uncertainty in the voltage supplied is 4.55% whereas the mass flow rate uncertainty is 2.46%. The range of instability is bounded for the lower part by the beginning of the unstable behavior. The higher zone corresponds to the end of the unstable behavior observed. These thresholds are materialized by a continuous lower line and a dashed upper line. So, the unsteady zone can be located in a specific area in a diagram using these two parameters. This classical way to locate the unstable area is completed by Fig. 4. The oscillation frequency of operating conditions previously presented as a function of the vapor quality is presented in a non-dimensional form in Fig. 4. The uncertainty in the non-dimensional frequency ($F.\tau$) is 2.42% and that in the exit vapor quality ($\chi_V$) is 8.73% due to the sum of the uncertainties in the mass flow rate, the heat flux, the channel length and hydraulic diameter. There appears a global increasing evolution of the non-dimensional frequency with the exit vapor quality whatever the mass flow rate.

The transit time of a liquid particle from the inlet to the outlet of the channel ($\tau$) is used to normalize the frequency and obtain a relation which links the oscillation frequency to the exit vapor quality. This result shows a general correlation, the constant ($k = 19.6$) is linked neither to the heat flux nor to the mass flow rate. $k$ only depends on the physical parameters and the channel geometry. Such a law can be explained by a local approach. A high exit-vapor quality corresponds to a high bubble-generation rate. It will be seen in a later section (Section 3.5.1) that the two-phase flow behavior consists of bubble expansion in the channel. If the mass flow rate is constant, an increase in heat flux will induce a higher exit-vapor quality. The same result can be obtained at a constant heat flux by reducing the mass flow rate. The common consequence will be a higher vapor

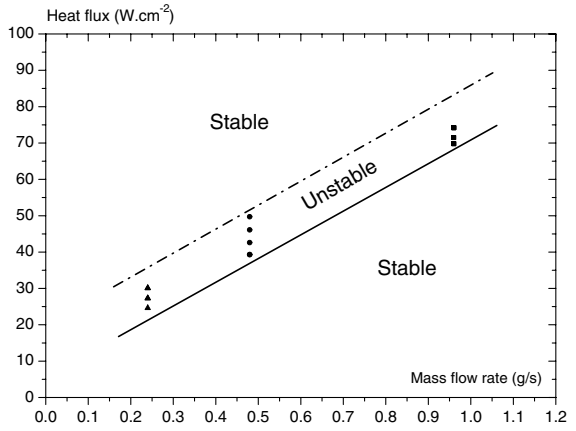


Fig. 3. Stability diagram of heat flux supplied as a function of the mass flow rate of a $0.5 \times 4 \times 50$ mm$^3$ minichannel.

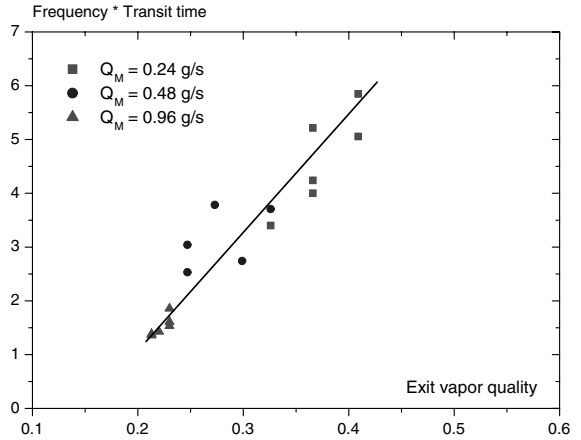


Fig. 4. Oscillation frequency by transit time of a liquid particle in the minichannel as a function of exit-vapor quality for different mass flow rates ($A = 2 \times 10^{-6}$ m$^2$, $L = 50$ mm).

Fig. 5. Picture of typical steady boiling occurring in a $0.5 \times 4 \times 200$ mm minichannel ($Q_M = 240$ kg m$^{-2}$ s$^{-1}$, $Q_W = 3.3 \times 10^4$ W m$^{-2}$).

rate generation and so a higher bubble generation frequency.

### 3.4. Steady-state-flow boiling analysis

As explained previously, for a given mass flow rate and below a critical heat-flux, flow boiling is steady following the criterion defined in Section 3.2. In Fig. 5 flow boiling is under steady conditions ($(e, l, L) = 0.5 \times 4 \times 200$ mm$^3$, $Q_M = 240$ kg m$^{-2}$ s$^{-1}$, $Q_W = 3.3 \times 10^4$ W m$^{-2}$). Bubbles created at the beginning of the two-phase area evolve and grow to reach the channel cross-section. The field of view is 4 mm wide by 80 mm long beginning at the abcissa 15 mm from the entrance ($X = 0$ mm). The typical pressure and temperature signals corresponding to this behavior are presented in Figs. 6 and 7. The average pressure loss of 3090 Pa is disturbed by a fluctuation of amplitude less than 1000 Pa due to the bubble passage in front of the pressure sensors. The same behavior is observed in ducts with hydraulic diameters of a few centimeters [9].

The average temperature difference between the liquid at the outlet and the inlet of the channel depends on the operating conditions and the spectral analysis does provide any characteristic frequency. On average, the exit pressure fluctuations are null but present a periodic characteristic behavior. The Fourier transform of the signal shows two frequencies with low amplitudes (20 rms(Pa$^2$)), which seem to correspond to the characteristic time of bubble passage in front of the exit pressure sensor (Fig. 8). The presence of two frequencies seems to indicate two separate kinds of bubbles which pass in front of the sensors. This is confirmed by the video analysis and more especially in Fig. 9. Small bubbles flowing near the channel sides are faster than huge bubbles flowing slowly in the middle of the channel. Their characteristic times of passage in front of the exit pressure sensor explain the two frequencies of Fig. 8. The small bubbles which evolve quickly will imply a high frequency around 20 Hz and the huge bubbles, a frequency around 5 Hz.

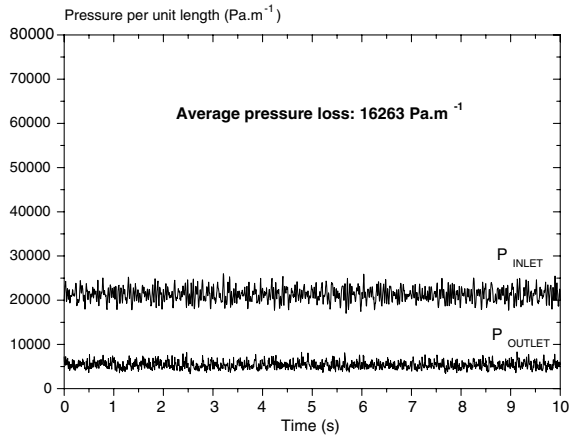


Fig. 6. Typical steady boiling inlet and outlet pressure signals ($D_H = 888.9$ μm, $L = 200$ mm, $Q_M = 240$ kg m$^{-2}$ s$^{-1}$, $Q_W = 3.3 \times 10^4$ W m$^{-2}$).

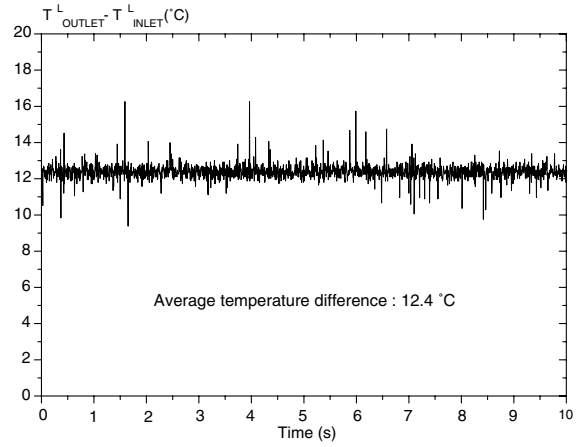


Fig. 7. Typical steady boiling temperature difference [$(e, l, L) = 0.5 \times 4 \times 200$ mm$^3$, $Q_M = 240$ kg m$^{-2}$ s$^{-1}$, $Q_W = 3.3 \times 10^4$ W m$^{-2}$].

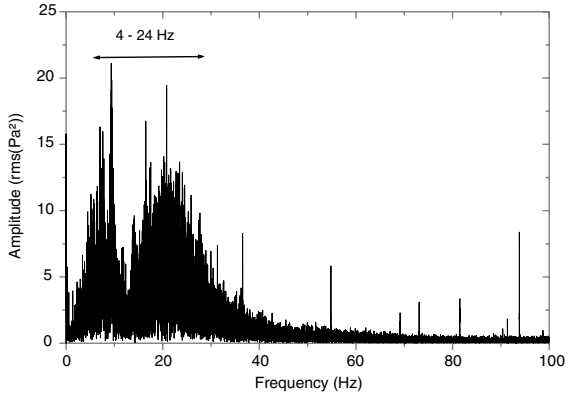


Fig. 8. Spectrum analysis of an outlet pressure signal in a steady boiling state (signal in Fig. 6).

Fig. 9. Typical steady boiling with two characteristic bubble diameters in a $0.5 \times 4 \times 200$ mm$^3$ minichannel ($Q_M = 240$ kg m$^{-2}$ s$^{-1}$, $Q_W = 3.3 \times 10^4$ W m$^{-2}$).

### 3.5. Unsteady-flow-boiling analysis

#### 3.5.1. Behavior analysis

The experimental conditions to perform the video acquisition are the same thermo-hydraulic parameters as for the steady state (Section 3.4) except for the heat flux provided to the channel which is multiplied by 3 ($Q_W = 9.6 \times 10^4$ W m$^{-2}$), the video camera is a: Fastcam® Ultima Series IEEE 1394, with an acquisition frequency of 1000 frames/s and a shutter of 250 μs. The pressure measurements (inlet and outlet) are taken through the transparent front face at the abscissa $X = 0$ mm and $X = 200$ mm. There is no synchronization between pressure measurements and visualization. Coupling between the signal and video is done by determining a reference (Point B). At point B, the upstream two-phase flow is stopped and corresponds to the maximum pressure in the inlet.

The pressure signal of this unsteady flow in Fig. 10 is to be compared to steady-flow-boiling. The average pressure drop is much higher than that of the steady situation. Furthermore, the inlet pressure signal presents a regular pattern of high amplitude (8 kPa) and low frequency (~4 Hz and high peak amplitude 3000 rms(Pa$^2$)). The corresponding spectrum analysis in Fig. 11 shows a main oscillation frequency at 3.59 Hz and 2 harmonics. The outlet pressure signal also presents characteristic behavior with a low oscillation amplitude (<2 kPa). A spectrum analysis indicates the same oscillation frequency as the inlet pressure signal with a smaller peak amplitude 80 rms(Pa$^2$). There is a straightforward explanation for the higher amplitude of pressure oscillation at the channel inlet. In Eqs. (2) and (3), the outlet and inlet pressure terms are given. The outlet pressure is mainly due to the dynamic term of the two-phase flow speed (first part) and secondarily due to the static pressure of the two-phase flow between the channel exit and the separator. The inlet pressure is the sum of four terms: the pressure loss due to the liquid, biphasic and vapor (if the latter exists) zones plus the outlet pressure term.

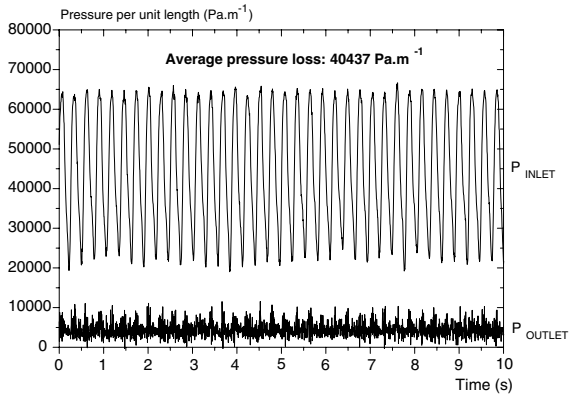


Fig. 10. Typical unsteady boiling inlet and outlet pressure signals ($D_H = 888.9$ μm, $L = 200$ mm, $Q_M = 240$ kg m$^{-2}$ s$^{-1}$, $Q_W = 9.6 \times 10^4$ W m$^{-2}$).

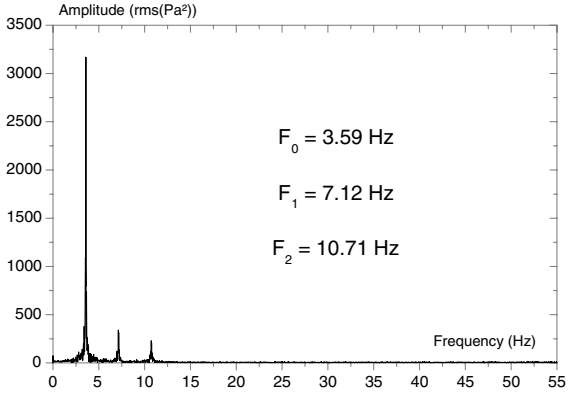


Fig. 11. Spectrum analysis of a typical unsteady pressure loss (signal in Fig. 10).

$$P_{In} = \Delta P_L + \Delta P_B + \Delta P_V + P_{Out} \quad (2)$$

$$P_{Out} = \tfrac{1}{2}\varrho_{Out} U_{Out}^2 + \varrho_{Out} g d_{Out} + P_{Atm} \quad (3)$$

A first order stability analysis shows that the inlet pressure oscillation amplitude is related to the outlet one by Eq. (4). The inlet pressure will then have an oscillation amplitude higher than the outlet one. The biphasic zone due to vapor compressibility will have a higher potential of compression and thus a higher oscillation amplitude. The liquid pressure fluctuation will be smaller without any available compressibility and the vapor term will also be small due to the exit to the atmospheric pressure in the separator which can be considered as a huge tank (vibration-reducer).

$$\frac{\delta P_{In}}{\delta P_{Out}} = 1 + \frac{\delta P_L + \delta P_B + \delta P_V}{\delta P_{Out}} \quad (4)$$

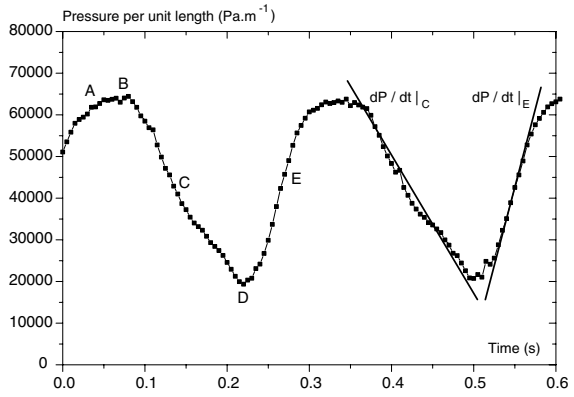


Fig. 12. Typical outlet pressure signal during unsteady boiling shown over two periods ($D_H = 888.9$ μm, $L = 200$ mm, $Q_M = 240$ kg m$^{-2}$ s$^{-1}$, $Q_W = 9.6 \times 10^4$ W m$^{-2}$).

To analyze the two-phase flow behavior, we describe below the different steps observed during one period (Fig. 12):

- Liquid flows in the channel (Point A). Bubbles are created at the beginning of the two-phase flow zone. Their size and generation rates are such that bubbles coalesce to vapor slugs which evolve in the channel. Vapor slugs generate over-pressure which reduce the upstream boiling flow rate.
- Bubbles growing before the vapor slug slow down, stop (Point B) and quickly reach the entire channel cross-section. Vapor created by bubble expansion must be evacuated; but downstream in the channel vapor slugs block the flow.
- Expanding vapor pushes the inflow back to the entrance using the buffer tank as a mass flow storage (Point C).
- Finally the channel is fully of vapor (Point D). The surface temperature rises due to the heat flux permanently provided to the fluid and not removed by boiling.
- When the channel is empty and upstream pressure before the channel entrance is sufficient, the entire vapor slug which occupies the channel is expelled. The channel is refilled with liquid (Point E).
- Due to the high surface temperature, bubbles are quickly formed (Point A) and the phenomenon is again repeated.

If we look at the pressure evolution in Fig. 12, we observe in one period three distinct parts (about 275 ms). The first one consists of the pressure decrease during approximately 150 ms from B to D; the average pressure decrease in C at 62 kPa s$^{-1}$ whereas in the second part the liquid refilling with a duration of about 65 ms corresponds to the D–A part on the curve. The average pressure increase in E is about 136 kPa s$^{-1}$. The third part between A and B flowing in the channel and slowing down is only 60 ms of one period.

### 3.5.2. Back-flow behavior

In the B–D part of Fig. 12, vapor expands up to the channel entrance and exit. Fourteen pictures (Fig. 13) have been selected to analyze the phenomena occurring in the channel from the previous section (Section 3.5.1). The outline of a few bubbles is chosen to follow their evolution inside the channel. With the first three pictures (Point A in Fig. 12), the bubble evolution in the channel is observed at about the velocity of the inlet liquid whereas between the fourth and the fifth they are quite static and grow (Point B in Fig. 12). With the last nine pictures, the slug formation and expansion to the entrance and to the exit is clear. The channel in the last

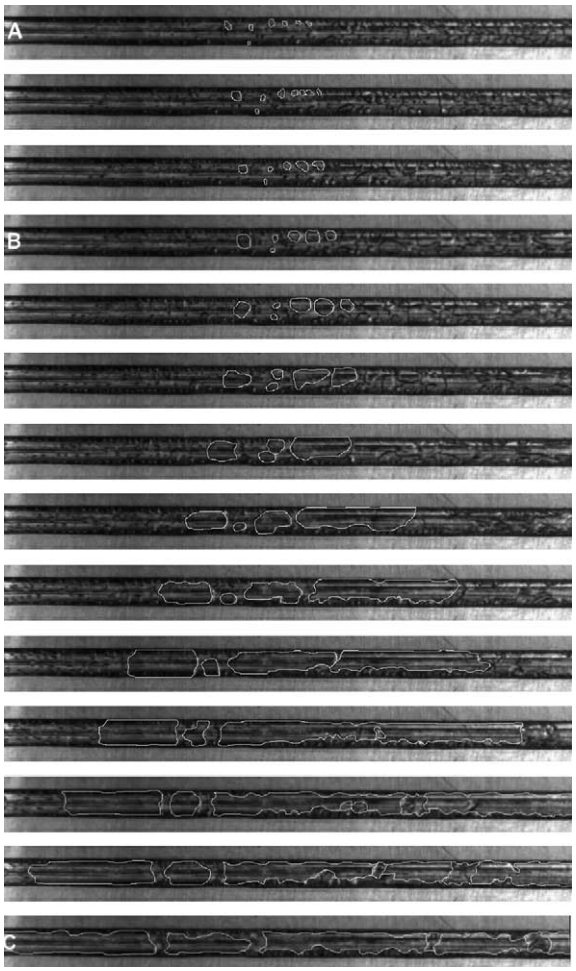


Fig. 13. Vapor slug formation during flow boiling: example of backflow [5 ms between two pictures] (some bubble outlines were evidenced to follow their evolution).

picture is solely vapor and few liquid zones remain. The vapor expansion to the entrance is possible by the fluid reverse flow into the buffer tank. It can be seen that vapor propagation is faster downstream than upstream due to the higher outgoing vapor quality. In fact, the downstream pressure drop is small enough to allow quick vapor expulsion whereas the upstream vapor expansion is conditioned by the buffer tank compliance.

The entire movies are available on: http://iusti.univ-mrs.fr/IUSTI/Equipes/Tcm/membres/Doctorants/dbrutin/dbrutin.htm

## 4. Conclusion

An experimental device to investigate two-phase flow instabilities in narrow channels was designed and the presence of a two-phase flow oscillation phenomena occurring in flow boiling was evidenced. An analysis of the steady and unsteady behavior is made through a flow pattern analysis and a stability delimitation of the unsteady zone. Video analysis of a reverse flow for an unsteady period is also proposed. This phenomenon shows the vapor slug formation which blocks the two-phase flow and pushes the two-phase flow back to the entrance. This work will be extended by a model for a better understanding of the loop-channel coupling and by an analysis of the upstream and downstream conditions' influence on the unsteady behavior.

## References

[1] K.S. Roy, B.L. Avanic, A very high heat flux microchannel heat exchanger for cooling of semiconductor laser diode arrays, IEEE Transactions on components, packaging, and manufacturing technology 19B (May) (1996) 444–451.

[2] L.G. Neal, S.M. Zivi, The stability of boiling-water reactor and loops, Nuclear Science and Engineering 30 (1967) 25–38.

[3] J.A. Bouré, A. Mihaila, The oscillatory behavior of heated channels, in: Symp. on two-phase flow dynamics, Eindhoven, September 1967, pp. 695–720.

[4] A.H. Stenning, T.N. Veziroglu, Flow oscillation modes in forced convection boiling, in: Heat Transfer and Fluid Mechanics Institute, Los Angeles, 1965, pp. 301–316.

[5] A.H. Stenning, T.N. Veziroglu, G.M. Callahan, Pressure drop oscillations in forced convection flow with boiling, in: Symp. on two-phase flow dynamics, Eindhoven, September 1967, vol. 1, pp. 405–427.

[6] J.E. Kennedy, G.M. Roach, M.F. Dowling, S.I. Abdel-Khalik, Z.H. Quershi, S.M. Ghiaasiaan, S.M. Jeter, The onset of flow instability in uniformly heated horizontal microchannels, Journal of Heat Transfer 122 (February) (2000) 118–125.

[7] S.G. Kandlikar, in: Fundamental issues related to flow boiling in minichannels and microchannels, Experimental Heat Transfer, Fluid Mechanics, and Thermodynamics—ExHFT-5, Vol. 1, Edizioni ETS, Pisa, 2001, pp. 129–146.

[8] M. Ledinegg, Instability flow during natural forced circulation, Warme 61 (8) (1938) 891–898.

[9] A.E. Bergles, Review of instabilities in two-phase systems, in: Proceedings of NATO Advanced Study Institute, editor, Two-phase flow and heat transfer, pp. 383–423.

[10] G. Yadigaroglu, A.E. Bergles, Fundamental and higher-mode density-wave oscillations in two-phase flow, Journal of Heat Transfer 94 (1972) 189–195.

[11] R. Stelling, E.V. McAssey, T. Dougherty, B.W. Yang, The onset of flow instability for downward flow in vertical channels, Journal of Heat Transfer 118 (3) (1996) 709–714.

[12] S. Nair, S. Lele, M. Ishii, S.T. Revankar, Analysis of flow instabilities and their role on critical heat flux for two-phase downflow and low pressure systems, International Journal of Heat and Mass Transfer 39 (1) (1996) 39–48.

[13] P.A. Kew, K. Cornwell, Confined bubble flow and boiling in narrow spaces, in: 2nd Int. Heat Transfer Conference, Brighton 7, 1994, pp. 473–478.

[14] P.A. Kew, K. Cornwell, On pressure fluctuations during boiling in narrow channels, in: 2nd European Thermal-Sciences and 14th UIT National Heat Transfer Conference, 1996, pp. 1323–1327.

[15] M. Aligoodarz, Y. Yan, D. Kenning, Wall temperature and pressure variations during flow boiling in narrow channels, in: IHTC 11, Séoul, Korea 2 (1998) 225–230.

[16] X.F. Peng, B.X. Wang, Forced-convection and boiling characteristics in microchannels, in: IHTC 11, Séoul, Korea, 1998, pp. 371–390.

[17] L. Jiang, M. Wong, Y. Zohar, Phase change in micro-channel heat sink under forced convection boiling, in: 13th Annual International Workshop on micro electro mechanical systems 2000, pp. 397–402.

[18] Y. Chang, S. Yao, Pool boiling heat transfer in confined space, International Journal of Heat and Mass Transfer 26 (6) (1983) 841–848.

[19] M.W. Wambsganss, J.A. Jendrzejczyk, D.M. France, Determination and characteristics of the transition to two-phase slug flow in small horizontal channels, Journal of Fluid Engineering 116 (1994) 140–146.